Evidence for Direct Optical Interband Transitions in Isochromat Spectra from Pt Single-Crystal Surfaces

G. Denninger and V. Dose
Physikalisches Institut der Universität, D-8700 Würzburg, Germany

and

H. P. Bonzel
Institut für Grenzflächenforschung und Vakuumphysik der Kernforschungsanlage Jülich, D-5170 Jülich, Germany
(Received 2 December 1981)

Bremsstrahlung isochromat spectra at $\hbar\omega \cong 9.7$ eV were recorded from well characterized, clean Pt(111), Pt(100)1×1, and Pt(210) surfaces. These spectra show intense emission peaks at the Fermi level as well as smaller peaks whose positions and intensities vary with the orientation of the substrate and the angular range of the incident electrons. The large peaks at the Fermi level are due to the high density of unoccupied 5*d* states. The orientation-dependent peaks are assigned to direct optical interband transitions between unoccupied states.

PACS numbers: 71.20.+c, 71.25.Pi, 73.20.Cw, 79.60.Cn

The occupied part of the valence-band structure of transition metals has been extensively studied by photoemission spectroscopy, both in the x-ray (x-ray photoemission spectroscopy, XPS) and the ultraviolet (ultraviolet photoelectron spectroscopy, UPS) regions. It has been recognized that XPS data represent by and large the density of occupied states[1] whereas the emission features of angle-resolved UPS can be understood in terms of direct transitions between initial (occupied) and final (empty) states.[2] Through the variation of photon energies (20–160 eV) it has even become possible to map out experimental band structures for some metals along high-symmetry directions.[3–5] By analogy, the inverse process to photoemission, bremsstrahlung isochromat spectroscopy (BIS), has been utilized to measure the density of unoccupied states above the Fermi level for $\hbar\omega \geq 1000$ eV.[6,7] On the other hand, by detecting photons at lower energy, e.g., in the range 10–50 eV, it should also be possible to obtain features in the BIS data which arise from direct transitions between initially empty bands.[8,9] This latter point is the subject of our study.

In this Letter we present isochromat spectra for $\hbar\omega = 9.7$ eV taken from clean and well-characterized Pt(111), Pt(100)1×1, and Pt(210) surfaces. These spectra, although measured for a nonparallel incident electron beam, show considerable dependence on the crystallographic orientation and are thus the first evidence of band-structure effects in BIS. By comparing spectra taken with two different incident-electron angular spreads for each crystal orientation, we are able to correlate observed emission peaks with direct interband transitions between unoccupied states. The experimental setup for obtaining isochromat spectra is as follows: The Pt single crystal is sitting opposite to a directly heated W filament at a distance of 0.4 mm. Electrons are accelerated towards the Pt with a current density of about 1 mA/cm^2. Emitted photons of 9.7 ± 0.28 eV energy are detected within a solid angle of 0.35 sr normal to the Pt surface. A typical spectrum covers an energy range of 14 eV and takes about 3 min to record. Further experimental details concerning BIS have been published elsewhere.[10] The Pt crystals were cleaned by Ar sputtering and heating in O_2 until no contaminants could be detected by Auger-electron spectroscopy.[11] The Pt(100)1×1 structure was prepared in the manner described by Bonzel *et al.*[12] All Pt surfaces showed sharp low-energy electron-diffraction patterns with low background intensity.

The angular distribution of the incident electrons is, because of the particular geometric arrangement, quite broad. Figure 1(a) shows the calculated electron trajectories and the corresponding angular distribution in a plane perpendicular to the filament. The chosen geometry dictates a cutoff at 65°. The angular distribution in the plane containing the filament is narrower by roughly an order of magnitude and therefore negligible. In order to probe the influence of the angular distribution on the measured isochromat spectra, a repeller grid was mounted behind the W filament [see Fig. 1(b)] and operated at a negative bias relative to the filament. As a result the angular distribution of incident electrons becomes much narrower, as seen in Fig. 1(b). BIS

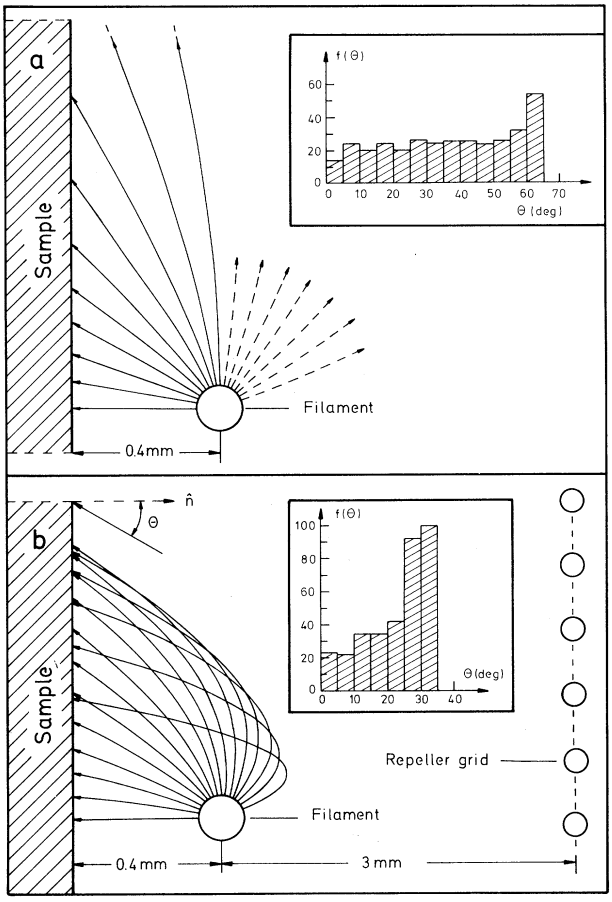

FIG. 1. (a) Electron trajectories calculated for the particular geometry of the experimental setup used in this work. The electron angular distribution as obtained from these trajectories is shown in the inset. (b) A repeller grid mounted behind the filament and operated at a negative bias with respect to the filament leads to a considerable narrowing of the angular distribution.

data will be presented for the two conditions defined by Fig. 1. All spectra were obtained in ultrahigh vacuum at $p \leq 5\times10^{-10}$ mbar.

The experimental isochromat spectra for the Pt(210), Pt(111), and Pt(100)1×1 surfaces and zero repeller bias are presented in Fig. 2. These spectra are characterized by a large photon emission peak at or slightly above the Fermi level, E_F, and smaller features at higher energies. These are superimposed on a rising background due to electron-hole-pair production.[13] There are considerable differences in the spectra illustrating the effect of crystallographic orientation.

With turned-on repeller bias and an electron angular distribution as displayed in Fig. 1(b) the

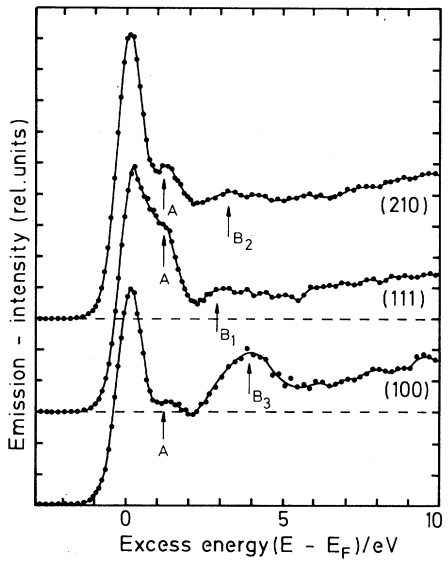

FIG. 2. Isochromat spectra for the Pt(210), Pt(111), and Pt(100)1×1 surfaces obtained with zero repeller bias, i.e., with an electron angular distribution as shown in Fig. 1(a), exhibit distinctly different structures superimposed on a smoothly varying background.

isochromat spectra changed to those shown in Fig. 3. The most apparent changes are a complete disappearance of peaks A and B_1 for the Pt(111), and a strong attenuation of peak B_3 for Pt(100) with an increase in peak A. The situation is reversed for the (210) surface, with peak A disappearing and enhanced emission from B_2. A more thorough investigation of the spectra reveals additional intensity variations at E_F.

The data presented in Figs. 2 and 3 can now be interpreted in the frame of the inverse photoemission picture.[8,9] The emission of photons occurs when incident electrons penetrate into the solid and undergo transitions from a high-lying initial state $|E\rangle$ to a low-lying final state $|\epsilon\rangle$ with $\epsilon = E - \hbar\omega$. The initial state can be a combination of exponentially decaying states (evanescent) and/or Bloch states. The transition probability depends on the density of initial and final states. The highest density of states exists for the empty Pt 5d band directly above the Fermi level. Transitions into this band can occur from Bloch as well as evanescent states causing strong photon emission. Thus the large peaks at E_F in Figs. 2 and 3 represent the empty Pt 5d-band density of states. Calculations by Larsson for normally incident electrons on Pt(100) and (111) surfaces are in agreement with this reasoning.[14]

The less intense features of the measured iso-

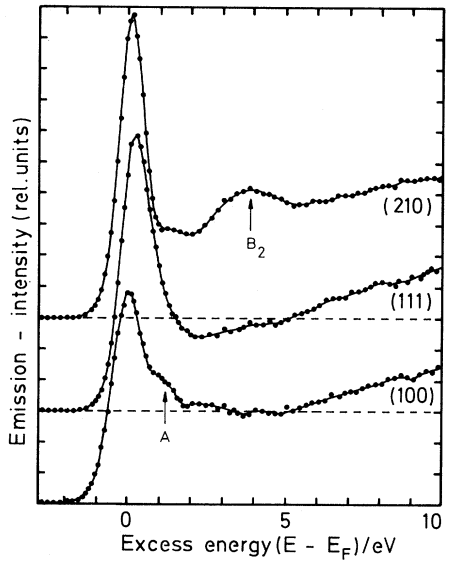

FIG. 3. Isochromat spectra obtained with negative bias applied to the repeller and an electron angular distribution as shown in Fig. 1(b). Note the complete disappearance of peaks A and B_1 for Pt(111), the strong attenuation of peaks A for Pt(210) and B_3 for Pt(100), and the enhancement of A for Pt(100) and B_2 for Pt(210).

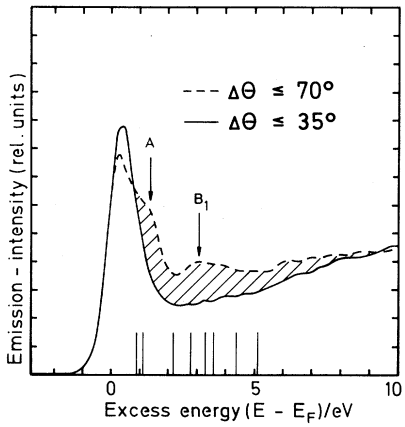

FIG. 4. Isochromat spectra for Pt(111) with and without negative bias on the repeller. The hatched area represents emission due to electrons with angles of incidence between 35° and 70°. Experimentally observed peaks are indicated by arrows whereas peak positions predicted from the band-structure analysis are indicated by the vertical bars.

chromat spectra can be correlated with direct transitions between Bloch states. In order to show this, we devised a procedure for obtaining sets of (ϵ, θ) values, where ϵ is the final-state energy of the electron and θ the angle of incidence of the primary electron. The procedure is complicated because of the somewhat disadvantageous geometry of the experiment. Since in all cases relatively large ranges of the angle of incidence are permitted (Fig. 1) it is necessary to probe large sections of the Brillouin zone for possible direct interband transitions. It is by no means sufficient to only check high-symmetry lines as it is commonly done in angular-resolved UPS.

In this procedure the band structure of Pt (Ref. 15) was analyzed for direct transitions with $\hbar\omega \cong 9.7$ eV. The results were initial and final-state energies as well as corresponding $\vec{k}$ vectors. The possible angles of incidence θ and Φ were calculated according to

$$k' = (2mE_{\text{kin}})^{1/2}/\hbar \quad (1)$$

$$k_x' = k' \sin\theta \cos\Phi = k_x \quad (2)$$

$$k_y' = k' \sin\theta \sin\Phi = k_y, \quad (3)$$

where $\vec{k}'$ is the $\vec{k}$ vector outside the solid. Only conservation of parallel momentum at the surface was assumed [Eqs. (2) and (3)], while no restriction in $k_\perp$ was imposed. The azimuth Φ was determined from the respective low-energy electron-diffraction pattern. Umklapp processes were permitted in that reciprocal lattice vectors were added to the $\vec{k}$ vectors determined from the band structure. In this manner the experimentally observable transitions were predicted for each crystal orientation. The results are illustrated by example of the Pt(111) crystal. Figure 4 shows a comparison of isochromat spectra for Pt(111) taken for the two angular ranges defined in Fig. 1. In this case it is particularly evident that a restriction in the allowed angular range of the incident electrons leads to a drastic elimination of extra emission features which are present for $\Delta\theta \leq 70°$. The analysis of the Pt band structure yields possible transitions at 0.9, 1.1, 2.2, 2.8, 3.3, 3.6, 4.4, and 5.1 eV with corresponding polar angles all above 60° (compare Table I). The transitions at 0.9 and 1.1 eV may be identified with the experimentally observed structure A while the remaining group covering the range from 2.2 to 5.1 eV is believed to be responsible for the rather broad structure B_1. The agreement in energetic position between theory and experiment is fairly good, particularly in view of the limited reliability of band-structure calculations for the unoccupied part of the conduction band. Since extra emissions A and B_1 result from electrons with polar angles $\theta \geq 60°$ they should disappear with the angular range restrict-

TABLE I. Direct radiative transitions predicted from an analysis of the theoretical band structure. The final-state energy of the electron relative to the Fermi level is given in the first column. The second column lists the reduced $\vec{k}$ vectors referred to a cubic cell. The last two columns give the polar angle θ and azimuthal angle Φ satisfying conservation of parallel momentum on the (111) surface.

Energy $E-\hbar\omega$ (eV)	Reduced $\vec{k}$ vector (in units of $2\pi/a$)	θ (deg)	Φ (deg)
0.93	(0.19, 0.31, $\overline{0.56}$)	62.8	7.6
1.1	(0.13, 0.19, $\overline{0.68}$)	63.4	3.7
2.2	(0.0, 0.19, $\overline{0.81}$)	63.3	10.2
2.8	(0.06, 0.13, $\overline{0.93}$)	73.4	3.0
	($\overline{0.06}$, 0.13, $\overline{0.93}$)	65.9	9.5
3.3	(0.13, 0.25, $\overline{0.81}$)	65.7	6.2
3.6	(0.06, 0.19, $\overline{0.94}$)	71.2	5.8
	($\overline{0.06}$, 0.19, $\overline{0.94}$)	64.6	12.2
	(0.13, 0.38, $\overline{0.75}$)	64.8	12.2
4.3	(0.19, 0.44, $\overline{0.75}$)	66.6	11.5
4.4	(0.06, 0.25, $\overline{0.94}$)	69.6	8.4
	($\overline{0.06}$, 0.25, $\overline{0.94}$)	63.6	14.7
5.1	(0.0, 0.31, $\overline{0.94}$)	66.0	13.9

ed to less than 60°. Figure 4 confirms that this is indeed the case.

The analysis is more complicated for the other two surfaces (100) and (210). This is largely because the chosen plane of incidence is not a mirror plane of the crystal. Measurements on these surfaces have therefore been taken with four different angular distributions. A detailed discussion of these results will appear elsewhere.[16]

In summary, first measurements of isochromat spectra from well-defined Pt single-crystal surfaces show considerable structure whose origin is crystallographic. Changes in the total angular range of incident electrons result in concomitant changes in the emission spectra. A first evaluation of the spectra by using a theoretical band structure of Pt provides evidence for direct interband transitions between unoccupied states. Therefore the first demonstration for the feasibility of angular-resolved isochromat spectroscopy is presented.

We would like to thank Dr. A. Liebsch and Dr. H. Scheidt for numerous helpful discussions and Dr. N. E. Christensen for sending us a printout of the Pt band structure.

[1]N. V. Smith, G. K. Wertheim, S. Hüfner, and M. M. Traum, Phys. Rev. B 10, 3197 (1974).

[2]C. N. Berglund and W. E. Spicer, Phys. Rev. 136, A1030 (1964); P. O. Nilsson and L. Ilver, Solid State Commun. 17, 667 (1975).

[3]J. Stöhr, P. S. Wehner, R. S. Williams, G. Apai, and D. A. Shirley, Phys. Rev. B 17, 587 (1978).

[4]D. E. Eastman, F. J. Himpsel, and J. A. Knapp, Phys. Rev. Lett. 40, 1514 (1978).

[5]F. J. Himpsel and D. E. Eastman, Phys. Rev. B 18, 5236 (1978).

[6]H. Merz and K. Ulmer, Z. Phys. 212, 435 (1968).

[7]M. Conrad, V. Dose, Th. Fauster, and H. Scheidt, Appl. Phys. 20, 37 (1979).

[8]A. Liebsch, private communication.

[9]J. B. Pendry, J. Phys. C 14, 1381 (1981).

[10]G. Denninger, V. Dose, and H. Scheidt, Appl. Phys. 18, 375 (1979).

[11]H. P. Bonzel, A. M. Franken, and G. Pirug, Surf. Sci. 104, 625 (1981).

[12]H. P. Bonzel, G. Brodén, and G. Pirug, J. Catal. 53, 96 (1978).

[13]V. Dose and G. Reusing, Appl. Phys. 23, 131 (1980).

[14]C. G. Larsson and P. O. Nilsson, Phys. Lett. 85A, 393 (1981).

[15]N. E. Christensen, private communication. The band structure was obtained by employing a relativistic linear combination of muffin-tin orbitals scheme. 505 $E(\vec{k})$ points in 1/48 Brillouin zone were available for our analysis.

[16]G. Denninger, doctoral thesis, University of Würzburg, Germany (unpublished).